Signals and Systems
Design of an autopilot

Laboratory Report

Imperial College London
Department of Aeronautics

Student: Xerxes Chong Xian

CID: 01389744

Laboratory Date: 21 February 2019

Submission Date: 22 March 2019

Table of Contents

1 Preparatory Exercise

1.1 System Identification

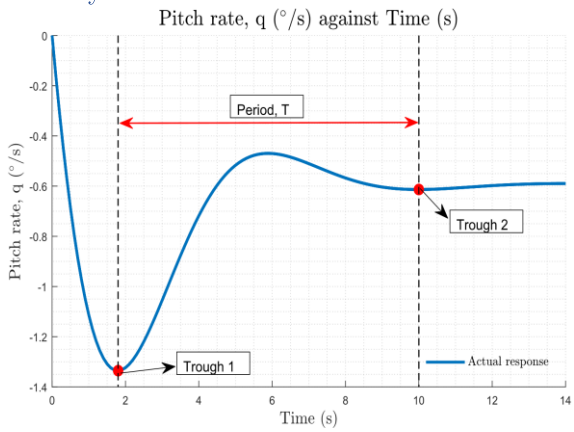

Figure 1-1 Pitch rate time response to step input on elevator

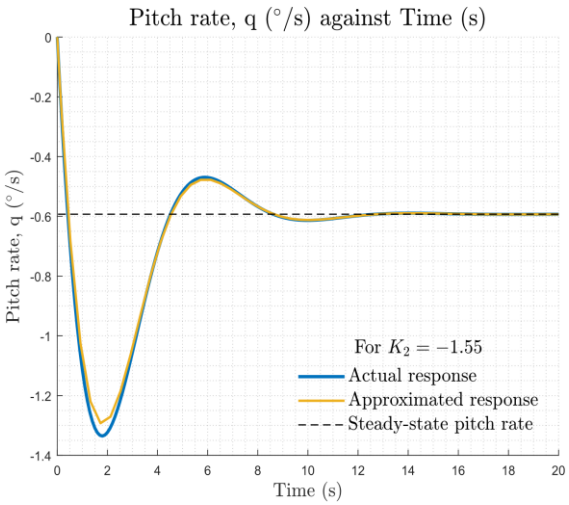

Figure 1-2 Linear model (approximated response) is matched to the actual response to obtain K_2

The response.mat file was plotted in Figure 1-1. From here the time between the 2 troughs were identified and this is the period, T found to be 8.2s. The pitch rate response eventually decayed to its steady-state, which corresponds to the parameter K_1, a value of -0.5929 rad/s. Using these constants, the damping ratio, ζ, and damped frequency, ω_d, can be found as shown in Table 1.

Table 1-1 Parameters of the transfer function

Parameter	Method	Value
K_1	$\lim_{s\to+0} c(t) = K_1$	-0.5929
ζ	$\frac{\zeta}{\sqrt{1-\zeta}} = \frac{1}{2\pi} ln\left(\frac{K_1 - c(t)}{K_1 - c(t+T)}\right)$	0.4955
ω_d	$\omega_d = \frac{2\pi}{T\sqrt{1-\zeta^2}}$	0.8822

$$G(s) = \frac{K_2 s - 0.4614}{s^2 + 0.8743s + 0.7782} \quad (1.1)$$

Applying the Laplace transformation to the second-order ordinary differential equation relationship between the elevator deflection and pitch rate, Equation 1.1 is obtained. This is the transfer function, G(s), in Equation 2 of (1) with the unknown parameter K_2. By method of trial and error, G(s) was tested at different values of K_2 and this approximated response was plotted alongside the response.mat data in Figure 2. From 0s to 8s, the approximated response is seen to deviate slightly especially at the trough and peak around 2s and 6s respectively. Beyond 6s, the approximated response was a good fit with a steady-state error of -5×10^{-4} °/s. Given the overall close matching of the plots and the low steady-state error. the value of $K_2 = -1.55$ adequately approximates the pitch rate response of the aircraft.

1.2 System Analysis and Control Design

$$\ddot{y}(t) - 3\dot{y}(t) = \dot{u}(t) + 2u(t) \xrightarrow{Laplace\ Transform} s^2L\{y\} - 3sL\{y\} = sL\{u\} + 2L\{u\}$$

$$L\{y\}(s^2 - 3s) = L\{u\}(s+2) \Rightarrow H(s) = \frac{Y(s)}{U(s)} = \frac{L\{y\}}{L\{u\}} = \frac{s+2}{s^2 - 3s} \quad (1.2)$$

Applying the Laplace transformation to the linear time-invariant LTI system with inputs u and y, the transfer function $\frac{Y(s)}{U(s)}$ is derived in Equation 1.2 above. This transfer function was then implemented at varying values of gain in the preparatory exercise system shown in Figure 2 of the handout (1).

In Figure 1-3a at a Gain of 1, the transfer function response is observed to oscillate between increasing values of amplitudes, never converging to a value. It is unstable at a Gain of 1. At a Gain of 10 in Figure 1-3b, the response peaks at a value of 1.3941 at 1.4673s before converging to unity at 4.1873s. The system can be concluded to be stable at Gain of 10. There is a Gain value at which the system transitions from unstable to stable. From trial and error, the transfer function response is observed to oscillate between a constant output at Gain ≈ 3.00 seen in Figure 1-4b. For Gain < 3.00, the amplitude of the response grows and diverges away from unity. This is observed in the diverging pattern seen in Figure 1-4a, where the Gain is 2.5. A larger growth rate of the response was also noted as Gain decreased from 3.00. For Gain > 3.00, the response decays and converges towards unity. This is observed in the converging pattern seen in Figure 1-4c, where the Gain is 3.01. A larger decay rate of the response was also noted as Gain increased from 3.00 The larger the gain, the greater the decay rate of the response. The system is therefore concluded to be stable, for a Gain > 3.00. This range of Gain will be important when the closed-loop transfer function of the system is considered below.

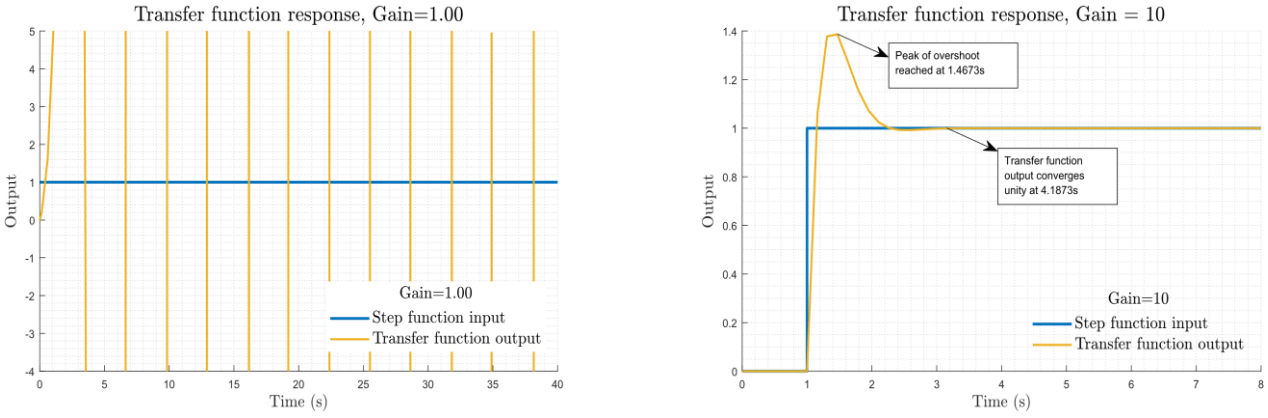

(a) (b)

Figure 1-3 Transfer function response compared with step function at Gains of 1 and 10

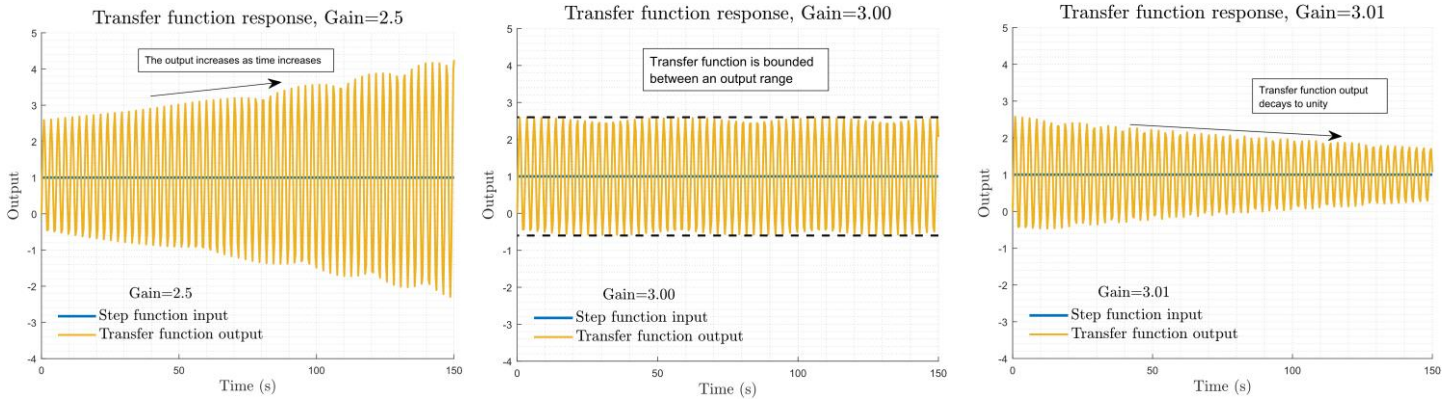

(a) (b) (c)

Figure 1-4 Changes in the shape of the open-loop transfer function response can be observed as the Gain increases past 3.00

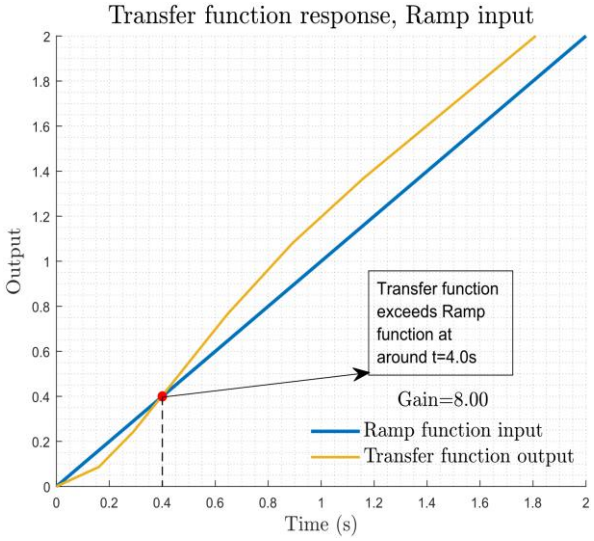

Figure 1-5 Transfer function response with a Ramp input. The gradient of the output matches the input after t=0.9s

$$Y(s) = KH(s)[U(s) - Y(s)]$$

$$\frac{Y(s)}{U(s)} = \frac{KH(s)}{1 + KH(s)} = \frac{K(s+2)}{s^2 + s(K-3) + 2K} \qquad (1.3)$$

From Figure 2.0 of the handout (1), the closed-loop relationship between the input and output of the system is derived above and re-arranged to obtain the closed-loop transfer function of the system, given $H(s) = \frac{s+2}{s^2 - 3s}$ from Section 1.2 and K being the Gain.

Table 1-2 Location of pole and zeroes for closed-loop transfer function

Zeroes	Poles
$s = -2$ *or* $K = 0$	$s = \frac{(3-K) \pm \sqrt{(K-3)^2 - 8K}}{2}$

The system has a zero when the numerator is 0 and a pole when the denominator is 0. For a system to be stable, $\mathrm{Re}(s) < 0$ so its pole lies in the negative region (left-hand side) of the complex plane and hence K > 3.0. This agrees with the range for Gain > 3.0 found earlier in Section 1.2. In Figure 1-5, the step input from Equation 1.3 was replaced with a ramp input. The transfer function output was then plotted against the input. The transfer function starts off lower than the ramp input but eventually overshoots it after t=0.4s, after which the gradients of both functions are equal. The distance between the 2 plots is the steady-state error. Subtracting the final value of both plots at t=150s, the steady-state error was found to be 0.1875. This value agrees with analytical solution to the steady state error found using Equation 1.4 from (2) below.

$$e(\infty) = \frac{1}{\left|\lim_{s\to 0} [s \times Gain \times Open\ loop\ Tran.Func]\right|} = \frac{1}{\left|\lim_{s\to 0} (s \times K \times H(s))\right|} = \frac{1}{\left|\lim_{s\to 0} \left[\frac{8(s+2)}{s-3}\right]\right|} = 0.1875 \qquad (1.4)$$

2 Main Lab

2.1 Pitch Controller Design and Implementation

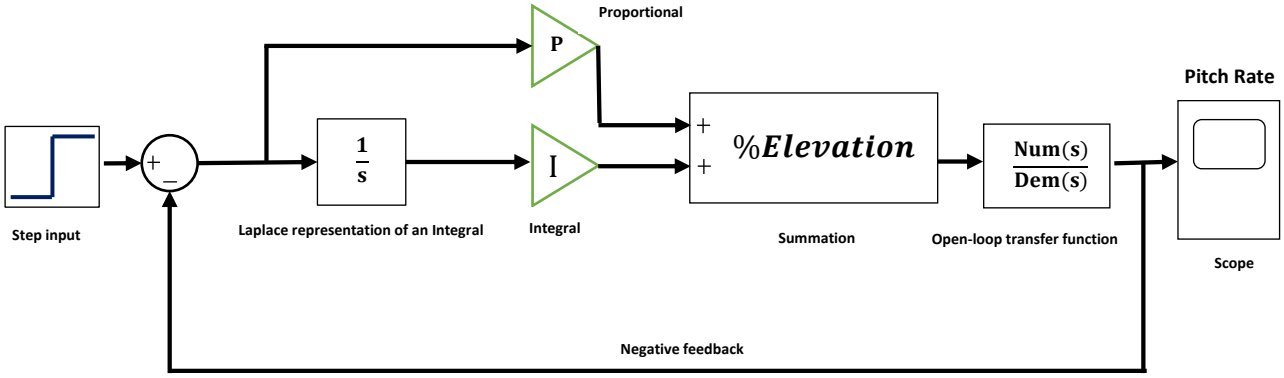

Figure 2-1 Block diagram of a PI controller for pitch rate regulation. It is like a PID diagram, with the derivative (D), K_d parameter set to 0

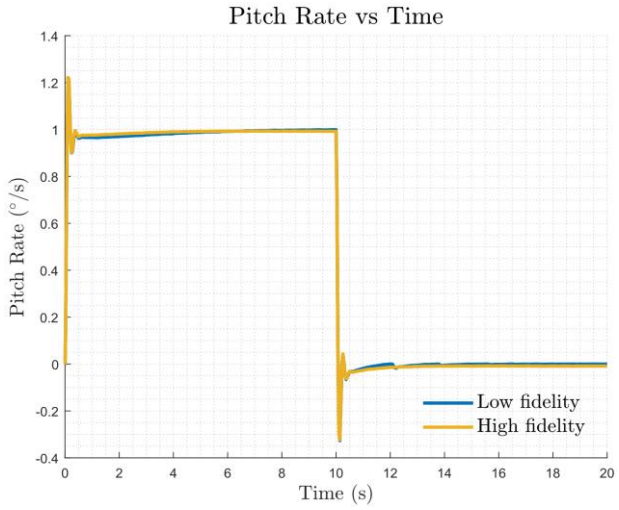

Figure 2-3 Comparing Pitch Rate vs Time between 2 models

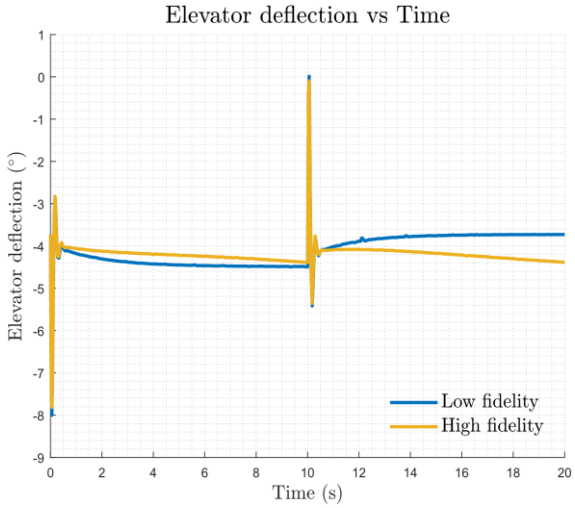

Figure 2-2 Comparing Elevator Deflection vs Time between 2 models

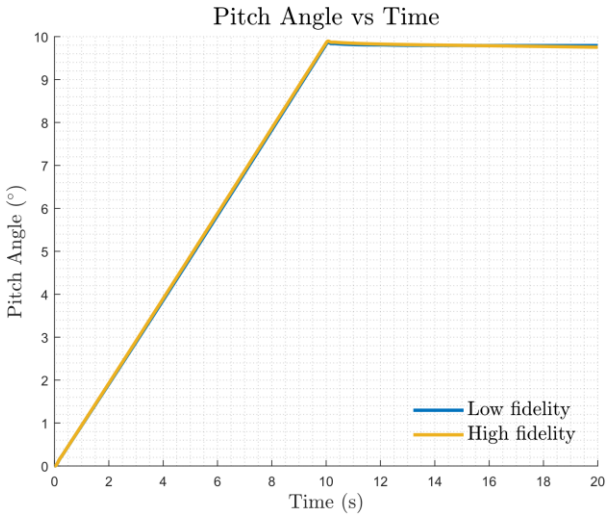

Figure 2-4 Comparing Pitch Angle vs Time between 2 models

Looking at Figure 2-2, Figure 2-3 and Figure 2-4, the low fidelity model matches the high fidelity model well. From t=0s to t=10s, all high-fidelity cases had a higher overshoot compared to the low fidelity. The low fidelity model is therefore an accurate approximation of the real response, though designers must consider the potentially dangerous of effects of having a slightly higher overshoot in the real system.

Table 2-1 Signal characteristics for low and high fidelity

	Low Fidelity	High Fidelity
Rise Time (s)	0.0403	0.0391
Settling Time (s)	1.2654	0.4281
Overshoot (%)	32.88	34.25
Steady-state error ($°/s$)	0.0008	0.0029

At t=0s, a deflection of the elevator induces a positive non-zero pitch rate, which changes the pitch angle of the aircraft. From t=0s to t=10s, the pitch rate is held at a constant as the pitch angle increase linearly. At about t=10s, the desired pitch angle of $\approx 10°$ is achieved, the elevator deflects in a range ≈ -4 to $0°$, causing the pitch rate to dip to zero, preventing any further changes to the pitch angle. It is likely this range of deflection induced a counter-acting pitch rate that reduces the positive pitch rate to zero, stopping the pitch angle from increasing. Using the stepinfo() function in MATLAB, the signal characteristics in Table 2-1 was obtained from the data in Figure 2-3 . K_i was decreased from -10 to -12, all other gains were unchanged when transitioning from the low to high fidelity simulations. The higher fidelity model's shorter settling and rise time, indicates the higher responsiveness of the real aircraft. Consequently, a higher overshoot is observed for the real aircraft. The steady-state error (steady-state value taken as 1.0) is nearly 4×

higher than the low fidelity model. This is in line with the decrease in K_i (3).

2.2 Airspeed Control Design and Implementation

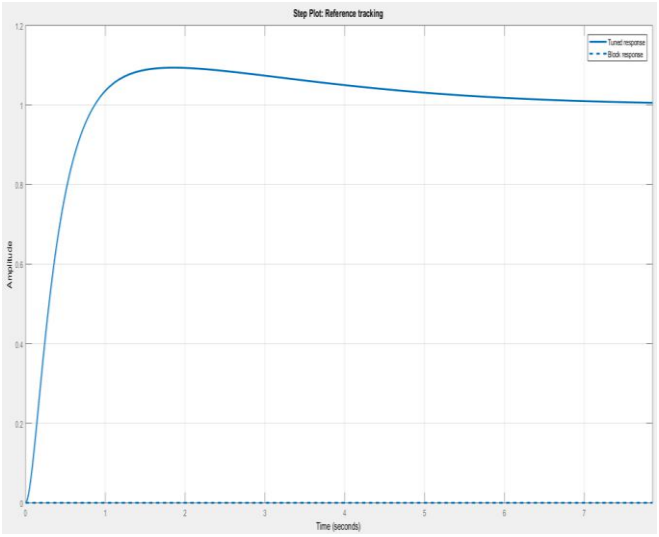

Figure 2-5 Screenshot of PID tuner. A plot of amplitudes vs time for the tuned response (solid blue line) of the airspeed controller

Table 2-2 Final airspeed PID controller gain values

K_p	K_i	K_d	N
2062.16	649.17	1540.40	13.88

The final gain parameters of the PID airspeed controller is shown in Table 2-2. The priority was rise time reduction to <3.0s, as pilots will expect a quick response when throttling up and down. The tuner probably changed this by increasing K_p and K_i , which reduces the rise time of the system response (3). The values were then fine-tuned manually to obtain an overshoot of <10%. Designers must consider the effects of overshoot on the response of the system and find a balance of signal response characteristics that matches the system's need. For an aircraft throttle controller, overshoots can lead to sudden accelerations/decelerations that affect the comfort and safety of the aircraft.

$$K_p + K_i \frac{1}{s} + K_d \frac{N}{1 + \frac{N}{s}} \qquad (2.1)$$

$$K_p + K_i \frac{1}{s} + K_d s \qquad (2.2)$$

Equation 2.2 is the theoretical PID expression and Equation 2.1 is MATLAB's in-built function. The term $\frac{N}{1+\frac{N}{s}}$ in Equation 2.1 and the s term of the K_d parameter in Equation 2.2 both represent a derivative. In the form of Equation 2.1 it is implemented as a low-pass filter (indicated by the N terms, a filter coefficient) in a negative feedback loop with an integral term in the feedback. In the form of Equation 2.2, it is just a derivative. While the use of derivatives is fine in theory, the form of Equation 2.2 requires more mathematical operations and computer memory, hence it is not preferred as the filter and negative-integral-feedback form of Equation 2.1 will produce more efficient algorithms that also filters out noise in the system response.

2.3 Comparison of Flight Control Cases

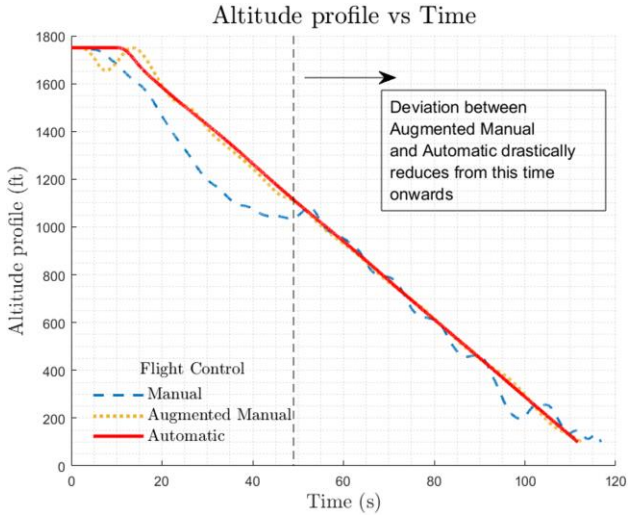

Figure 2-7 Altitude profile vs Time for all flight control cases

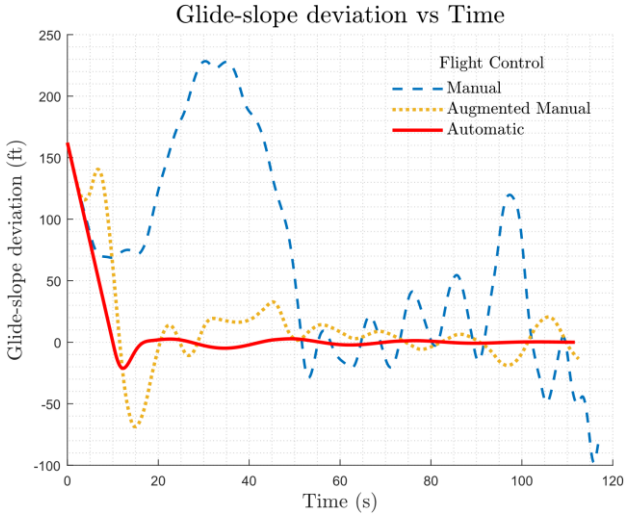

Figure 2-6 Glide-slope deviation vs Time for all flight control cases

From both figures above, the augmented manual control provided a vast improvement in handling of the aircraft over the manual control, with the automatic control deviating from the desired altitude profile and glide-slope the least. A decrease in the pilot-input was noted, transitioning from manual to automatic. The manual case in Figure 2-6 shows the tendency for the aircraft to oscillate about the desired glide-slope, especially from t=50s to t=110s. Hence, it is concluded that an increase in pilot-input promotes pilot-induced oscillation. As such oscillations can compromise the safety and comfort of the flight, this conclusion reiterates the need for an automatic control system.

Bibliography

1. **G.Papadakis.** *Signals and Systems Laboratory.* Department of Aeronautics, Imperial College London. London : Imperial College London, 2019. Laboratory Handout.
2. **B.Messner, et al.** Extras: Steady-State Error. *Control Tutorials for MATLAB and Simulink (CTMS).* [Online] Carnegie Mellon University; University of Michigan; Detroit Mercy, 2014. [Cited: 19 3 2019.] http://ctms.engin.umich.edu/CTMS/index.php?aux=Extras_Ess.
3. **Thorlabs.** PID Tutorials. *Thorlabs.* [Online] [Cited: 19 3 2019.] https://www.thorlabs.com/tutorials.cfm?tabID=5dfca308-d07e-46c9-baa0-4defc5c40c3e.